Triad interactions in the dissipation range

By S. Kida[1], R. H. Kraichnan[2], R. S. Rogallo[3], F. Waleffe[4], and Y. Zhou[4]

Nonlocality of the triad interactions in the dissipation range of developed turbulence is investigated by numerical simulation and the quasi-normal theories. It is found that the energy transfer is dominated by nonlocal triad interactions over the wavenumber range $0.1 < k/k_d < 4$, where k_d is the Kolmogorov wavenumber. The nonlocality of the interaction has a close relation with the power of an algebraic prefactor of the exponential decay of the energy spectrum in the far-dissipation range.

1. Introduction

The triad interaction is the fundamental coupling among the various Fourier components of a turbulent velocity field and transfers energy predominantly from lower to higher wavenumbers. Properties of the triad interactions were studied by Kraichnan (1971) and have recently been analyzed numerically using data from numerical simulations (Domaradzki 1988; Yeung & Brasseur 1991; Domaradzki & Rogallo 1990; Ohkitani & Kida 1992) and by an analysis of interactions among helical waves (Waleffe 1992).

In the inertial range where the energy spectrum obeys the Kolmogorov $-5/3$ power form,

$$E(k) = C_K \epsilon^{2/3} k^{-5/3}, \tag{1.1}$$

where ϵ is the energy dissipation rate and C_K is the Kolmogorov constant (Kolmogorov 1941), the interaction is local in the sense that triad interactions of scale disparity (see (3.4) for definition) greater than 10 (100) contribute only 15% (1%) of the energy flux (Kraichnan 1971; Ohkitani & Kida 1992). Although the locality of the triad interaction is very weak, it is compatible with Kolmogorov's (1941) concept of local energy cascade.

The nature of triad interactions in the dissipation range is expected to be different from that in the inertial range because the energy spectrum decreases very rapidly (exponentially) in the dissipation range. In this paper, we investigate the interactions by analyzing numerical turbulence and by its comparison with the prediction of the quasi-normal closure theories.

1 Kyoto University - RIMS
2 Santa Fe, NM
3 NASA Ames Research Center
4 Center for Turbulence Research

2. Fundamentals

We consider the energy dynamics of the motion of an incompressible viscous fluid in an infinite domain. The equation of motion is written in the Fourier representation as

$$\frac{\partial}{\partial t}\tilde{u}_j(\mathbf{k}) = -\frac{\mathrm{i}}{2}P_{jkl}(\mathbf{k}) \sum_{\mathbf{p}+\mathbf{q}+\mathbf{k}=\mathbf{0}} \tilde{u}_k^*(\mathbf{p})\tilde{u}_l^*(\mathbf{q}) - \nu k^2 \tilde{u}_j(\mathbf{k}) + \tilde{f}_j(\mathbf{k}) \tag{2.1}$$

with the continuity equation

$$k_j\, \tilde{u}_j(\mathbf{k}) = 0, \tag{2.2}$$

where $\tilde{u}_j(\mathbf{k})$ is the x_j $(j = 1, 2, 3)$ component of the Fourier coefficient of velocity at wavevector $\mathbf{k}$,

$$P_{jkl}(\mathbf{k}) = k_k\left(\delta_{jl} - \frac{k_j k_l}{k^2}\right) + k_l\left(\delta_{jk} - \frac{k_j k_k}{k^2}\right) \tag{2.3}$$

is a third order tensor, ν is the kinematic viscosity, and $\tilde{f}_j(\mathbf{k})$ is the external forcing. Here the time argument t is omitted for brevity, the asterisk denotes the complex conjugate, and repeated subscripts are summed over 1 to 3.

The energy spectral density at wavevector $\mathbf{k}$,

$$E(\mathbf{k}) = \tfrac{1}{2}|\tilde{\mathbf{u}}(\mathbf{k})|^2 \tag{2.4}$$

evolves according to

$$\frac{\partial}{\partial t}E(\mathbf{k}) = T(\mathbf{k}) - 2\nu k^2 E(\mathbf{k}) + \mathrm{Re}\left\{\tilde{u}_j^*(\mathbf{k})\tilde{f}_j(\mathbf{k})\right\}, \tag{2.5}$$

which is derived by multiplying (2.1) by $\tilde{u}_j^*$ and taking the real part.

The first term on the r.h.s. of (2.5) represents the rate of energy transfer to the Fourier mode $\mathbf{k}$ through the nonlinear interactions with all the other modes, the second the energy dissipation by the viscosity, and the third the energy input by the external force.

The energy transfer function $T(\mathbf{k})$ is written as

$$T(\mathbf{k}) = \sum_{\mathbf{p},\mathbf{q}} T(\mathbf{k}|\mathbf{p},\mathbf{q}), \tag{2.6}$$

where

$$T(\mathbf{k}|\mathbf{p},\mathbf{q}) = -\tfrac{1}{2}\mathrm{Im}\left\{P_{jkl}(\mathbf{k})\tilde{u}_j(\mathbf{k})\tilde{u}_k(\mathbf{p})\tilde{u}_l(\mathbf{q})\right\}\delta_{\mathbf{k}+\mathbf{p}+\mathbf{q}} \tag{2.7}$$

is the triad energy transfer due to the interaction among three wavevectors $\mathbf{k}$, $\mathbf{p}$, and $\mathbf{q}$ that constitute a triangle $(\mathbf{k} + \mathbf{p} + \mathbf{q} = 0)$. Through a triad interaction, energy is exchanged among the three modes involved, with the total energy being conserved. That is, the following detailed balance of energy holds;

$$T(\mathbf{k}|\mathbf{p},\mathbf{q}) + T(\mathbf{p}|\mathbf{q},\mathbf{k}) + T(\mathbf{q}|\mathbf{k},\mathbf{p}) = 0. \tag{2.8}$$

Consequently, the sum of the energy transfer function over all the wavevectors vanishes,

$$\sum_{\mathbf{k}} T(\mathbf{k}) = \sum_{\mathbf{k},\mathbf{p},\mathbf{q}} T(\mathbf{k}|\mathbf{p},\mathbf{q}) = 0. \tag{2.9}$$

Since the flow field is statistically isotropic, it is convenient to average each term in (2.5) over spherical cells in the wavevector space. We introduce the band-averaged energy spectrum

$$\hat{E}(k)\Delta k = \sum_{k-\frac{1}{2}\Delta k \le |\mathbf{k}'| < k+\frac{1}{2}\Delta k} E(\mathbf{k}'), \tag{2.10}$$

the band-averaged energy transfer function

$$\hat{T}(k)\Delta k = \sum_{k-\frac{1}{2}\Delta k \le |\mathbf{k}'| < k+\frac{1}{2}\Delta k} T(\mathbf{k}'), \tag{2.11}$$

and the band-averaged forcing spectrum

$$\hat{F}(k)\Delta k = \sum_{k-\frac{1}{2}\Delta k \le |\mathbf{k}'| < k+\frac{1}{2}\Delta k} \mathrm{Re}\left\{\tilde{u}_j^*(\mathbf{k}')\tilde{f}_j(\mathbf{k}')\right\}. \tag{2.12}$$

The energy spectrum equation (2.5) is then written for the band-averaged quantities as

$$\frac{\partial}{\partial t}\hat{E}(k) = \hat{T}(k) - 2\nu k^2 \hat{E}(k) + \hat{F}(k). \tag{2.13}$$

The triad energy transfer function $T(\mathbf{k}|\mathbf{p},\mathbf{q})$ is also averaged over a spherical cell as

$$\hat{T}(k|p,q)(\Delta k)^3 = \sum_{\substack{k-\frac{1}{2}\Delta k \le |\mathbf{k}'| < k+\frac{1}{2}\Delta k \\ p-\frac{1}{2}\Delta k \le |\mathbf{p}'| < p+\frac{1}{2}\Delta k \\ q-\frac{1}{2}\Delta k \le |\mathbf{q}'| < q+\frac{1}{2}\Delta k}} T(\mathbf{k}'|\mathbf{p}',\mathbf{q}'). \tag{2.14}$$

The energy transfer function is then written as

$$\hat{T}(k) = (\Delta k)^2 \sum_{p,q} \hat{T}(k|p,q). \tag{2.15}$$

The detailed balance of energy (2.8) and the conservation of total energy by all the triad interactions (2.9) are written respectively as

$$\hat{T}(k|p,q) + \hat{T}(p|q,k) + \hat{T}(q|k,p) = 0 \tag{2.16}$$

and

$$\sum_{k} \hat{T}(k) = 0. \tag{2.17}$$

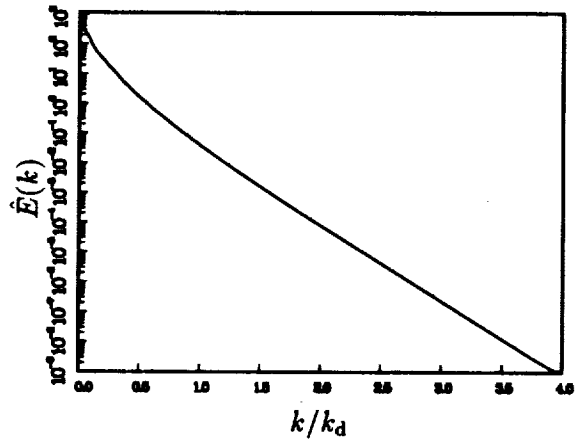

FIGURE 1. Energy Spectrum in the dissipation range. The decay with wavenumber is essentially exponential.

3. Numerical Simulation

The equations of motion (2.1) and (2.2) are solved numerically in a periodic cube with an instability forcing,

$$\tilde{f}_j(\mathbf{k}) = C\tilde{u}_j(\mathbf{k}) \qquad \text{for } |\mathbf{k}| \leq k_0. \tag{3.1}$$

The constant C is chosen to force the flow field to equilibrium with a specified range of forced scales $k_0 = 3$ and a specified range of resolved scales, in Kolmogorov units, $k_{max}/k_d = 4$. The Fourier-spectral method (Rogallo 1981) is employed for the spatial resolution, and time is advanced with a second-order Runge-Kutta procedure. The alias errors arising in the nonlinear terms is removed by a combination of coordinate shifting and spectral truncation. The computational mesh (in physical space) is 256^3. The initial flow field is taken after over five large-scale turnover times from forced turbulence created at a lower resolution (128^3) at about the same Reynolds number ($R_\lambda \approx 65$). The 256^3 field was then advanced until an equilibrium between transfer, and dissipation was achieved at the higher wavenumbers. We will study that transfer here in some detail. The Kolmogorov dissipation wavenumber,

$$k_d = (\nu^3/\epsilon)^{1/4} \tag{3.2}$$

is about 30, so that the maximum resolved wavenumber $k_{max} = 121$ retained in the simulation is about four times the Kolmogorov wavenumber.

3.1 Energy spectrum

The energy spectrum at the final time of the simulation is shown in a semi-logarithmic plot in figure 1. The nearly straight line indicates that the energy spectrum decays essentially exponentially with wavenumber. In order to examine

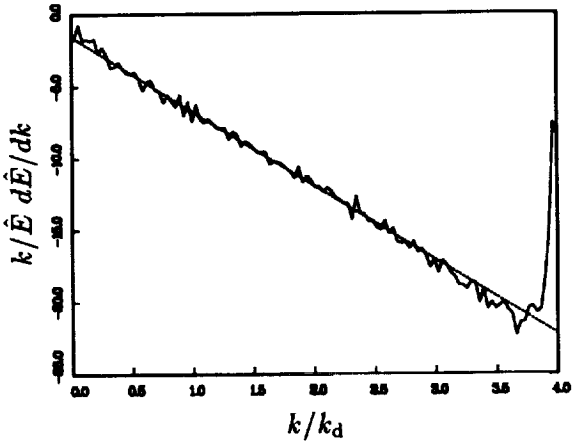

FIGURE 2. Logarithmic derivative of the energy spectrum function. For $E(k) = A(k/k_d)^\alpha \exp[-\beta k/k_d]$ the slope of the curve gives $-\beta$ and the intersection on the vertical axis gives α. ——— , simulation data; ---- , least-square fit over $.5 \leq k/k_d \leq 3$ gives $\alpha = -1.6$, $\beta = 5.2$.

the shape of the spectrum more precisely, we compare it with an exponential form with an algebraic prefactor

$$E(k) = A(k/k_d)^\alpha \exp[-\beta k/k_d]. \tag{3.3}$$

In figure 2, we plot the logarithmic derivative of the energy spectrum. If the spectrum has the form (3.3), the slope of the line and its intersection with the vertical axis give the values of β and α, respectively. Since this is an instantaneous spectrum, the fluctuations are quite large. Nevertheless, the least squares fit over $0.5 \leq k/k_d \leq 3$ gives $\alpha = -1.6$ and $\beta = 5.2$, which are consistent with those observed before in numerical simulations by other researchers (Kida & Murakami 1987; Kida *et al.* 1990; Kerr 1990; Sanada 1992). More recently however, Chen (1992 private communication) has simulated the dissipation range at $R_\lambda \approx 15$ to much higher k/k_d. He finds $\alpha = 2.16$ and $\beta = 7.35$ by a least-square fit over the range $5.2 \leq k/k_d \leq 10.4$. The data from the present simulations do not coincide with Chen's for $k/k_d \leq 4$, suggesting that the results are sensitive to Reynolds number. There may also be some effect due to the method of forcing. Incidentally, the exponential shape of the energy spectrum in the far-dissipation range has also been observed in experiments (Sreenivasan 1985).

There is a theoretical prediction of the power in the algebraic correction. The quasi-normal theories of turbulence (Kraichnan 1959; Tatsumi 1980; Lesieur 1987), which will be discussed in some detail in the next section, predict $\alpha = 3$ in the far-dissipation range. This value of α is quite different from those observed in the numerical simulations. But it should be remembered that the dissipation range is restricted to $k/k_d < 2 \sim 3$ in the simulations mentioned above so that it is not clear whether this discrepancy results from a failure of the quasi-normal theories

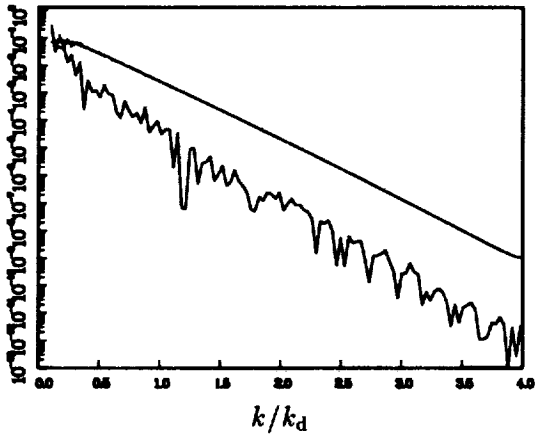

FIGURE 3. The energy-spectrum balance: ---- , transfer $\hat{T}(k)$; —·— , dissipation $2\nu k^2\hat{E}(k)$; ——— , departure from equilibrium $|\hat{T}(k) - 2\nu k^2\hat{E}(k)|$. The equilibrium between transfer and dissipation is apparent over most of the wavenumber range.

or from the low wavenumbers considered. As a matter of fact, there is a numerical suggestion that the spectrum may be consistent with positive values of α less than 3 over the wavenumber range $4 < k/k_d < 10$ for a low Reynolds number ($R_\lambda \approx 15$) flow (Domaradzki 1992 private communication).

In order to see the dominant terms of (2.13), we plot $\hat{T}(k)$ and $2\nu k^2\hat{E}(k)$ in figure 3. Recall that the forcing term $\hat{F}(k)$ in (2.13) is restricted to low wavenumbers ($k/k_d \leq 0.1$). We see that both $2\nu k^2\hat{E}(k)$ and $\hat{T}(k)$ vary exponentially with wavenumber and that they are in equilibrium. Their difference is less than their magnitude by more than two orders of magnitude over most of the wavenumber range ($k/k_d > 1$, say).

3.2 Triad energy transfer

The triad energy transfer function $\hat{T}(k|p,q)$ is most efficiently calculated by an alias-free spectral method applied to filtered fields (Domaradzki & Rogallo 1990). In figure 4, we plot $\hat{T}(k|p,q)$ for $k/k_d = 2$ and $k/k_d = 3$. The finest band-width is employed, i.e. $\Delta k = 1$. The solid and broken curves denote the positive and negative values, respectively. We recognize the following characteristics in $\hat{T}(k|p,q)$. First, there are strong dipoles at the corners $q \ll p \approx k$ and $p \ll q \approx k$ of the boundary. The signs of the dipoles are positive (negative) on the smaller (larger) side of wavenumber p/k or q/k. Second, the most significant part of $\hat{T}(k|p,q)$ is localized near the boundary $p + q = k$, and the thickness of this part decreases as k/k_d increases. The magnitude of $\hat{T}(k|p,q)$ decreases exponentially with wavenumber away from this boundary. The value of $\hat{T}(k|p,q)$ in the blank region is too low to draw clear curves.

The first characteristic was also observed in the inertial range (Kida & Ohkitani 1992) and represents the energy transferred to larger wavenumbers by nonlocal interactions. The second characteristic, on the other hand, is peculiar to the dissipation

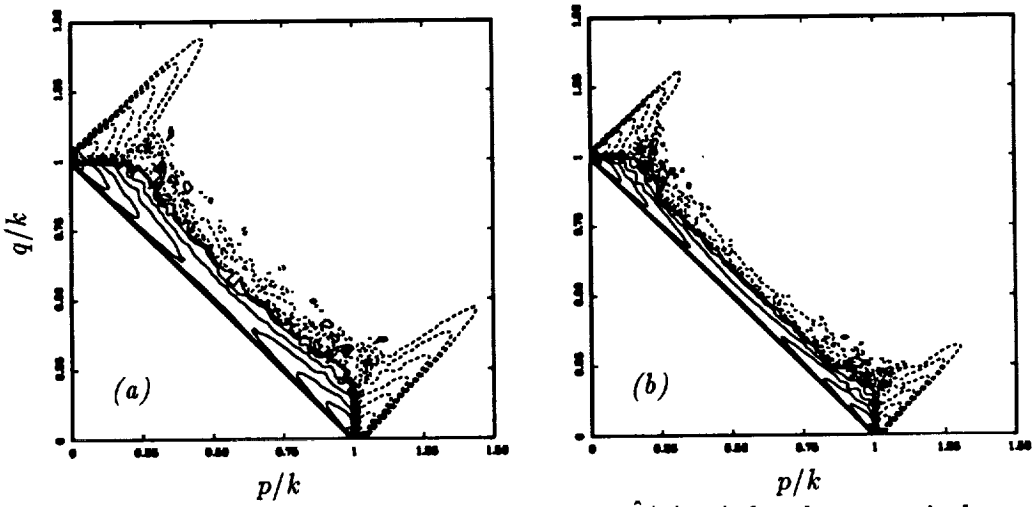

FIGURE 4. The triad energy transfer function $\hat{T}(k|p,q)$ for the numerical turbulence. (a) $k/k_d = 2$, (b) $k/k_d = 3$ The solid and broken curves represent the positive and negative parts, respectively. The contour levels are logarithmic, rather than linear, and are separated by a factor of 4.

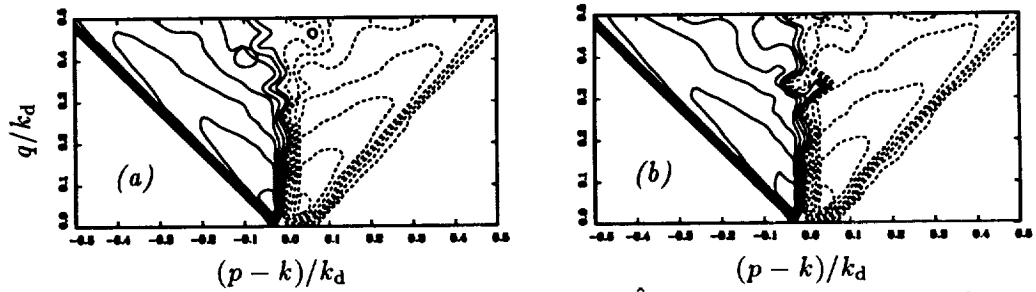

FIGURE 5. The triad energy transfer function $\hat{T}(k|p,q)$ for the numerical turbulence. (a) $k/k_d = 2$, (b) $k/k_d = 3$. The solid and broken curves represent the positive and negative parts, respectively. The contour levels are logarithmic, rather than linear, and are separated by a factor of 4.

range. This arises from the rapid (exponential) decay of the energy spectrum with wavenumber in the dissipation range in contrast with the slow (algebraic) decay in the inertial range.

Similarity in the contours evidently is not obtained over the whole domain of $\hat{T}(k|p,q)$ plotted in figure 4. Since, however, the dipole parts are very similar in figures 4(a) and (b), we enlarge the corner region and replot the contours in figures 5(a) and (b), respectively, with wavenumbers normalized by the Kolmogorov wavenumber k_d instead of k. This scaling of the wavenumber is suggested by the closure theory (see (4.12)).

The close resemblance of figures 5(a) and (b) implies that the shape of the dipoles of $\hat{T}(k|p,q)$ is similar near the corners if the wavenumber is scaled by the Kolmogorov wavenumber.

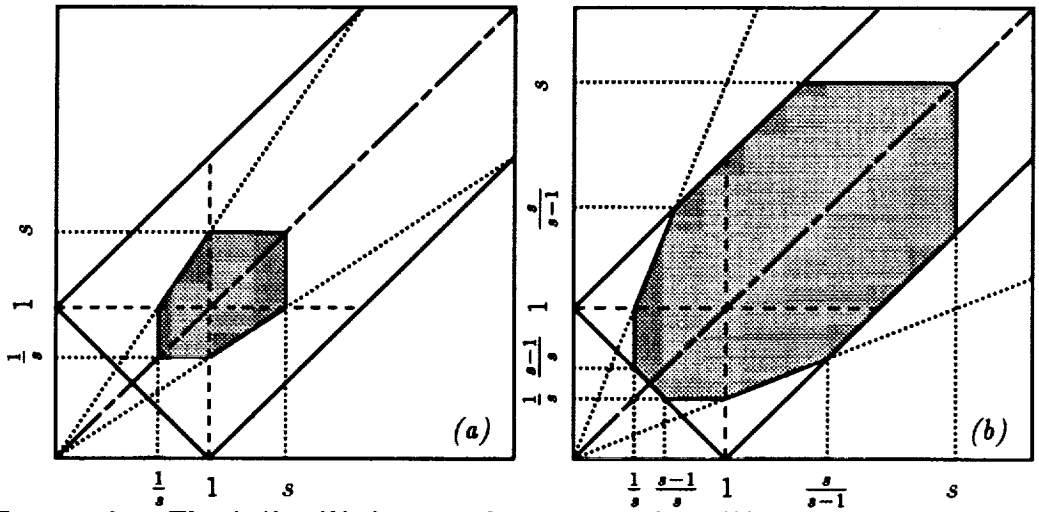

FIGURE 6. The $(p/k, q/k)$ domain of integration for $T(k|p,q)$. The measure of scale disparity is $s = \max(k,p,q)/\min(k,p,q)$. (a) $s \leq 2$, (b) $s \geq 2$.

3.3 Nonlocality of triad interaction

The triad energy transfer function $\hat{T}(k|p,q)$ represents the energy exchange among three wavenumbers with magnitudes k, p, and q. In order to express the scale locality of the triad interaction, we introduce the scale disparity parameter (Zhou 1992), the ratio of the maximum to the minimum of the triad wavenumbers,

$$s = \frac{\max(k,p,q)}{\min(k,p,q)}. \tag{3.4}$$

It follows by definition that $s \geq 1$. This scale disparity parameter measures the scale locality of the triad interaction. If s is smaller, the interaction is more local, and vice versa. In figure 6, we indicate the (k,p,q) domains for relatively local ($s \leq 2$) and relatively non-local ($s \geq 2$) triad interactions.

Let us denote by $\hat{T}(k|s)\Delta k$ the contribution to the energy transfer from triad interactions with scale disparity parameter between $s - \frac{1}{2}\Delta s$ and $s + \frac{1}{2}\Delta s$. Then, we have

$$\hat{T}(k|s) = (\Delta k)^2 \sum_{\substack{p,q \\ s-\frac{1}{2}\Delta s \leq \frac{\max(k,p,q)}{\min(k,p,q)} < s+\frac{1}{2}\Delta s}} \hat{T}(k|p,q). \tag{3.5}$$

In figure 7, we plot $\hat{T}(k|s)$, obtained by summing up the terms in the r.h.s. of (3.5) numerically for $k/k_d = 2$ and $k/k_d = 3$. It is seen that $\hat{T}(k|s)$ may have a scale similarity with sk_d/k.

4. Closure Theory

In the quasi-normal closure theories (see Tatsumi 1980; Lesieur 1987), the energy transfer term in the energy spectrum equation (2.13) is expressed in terms of the

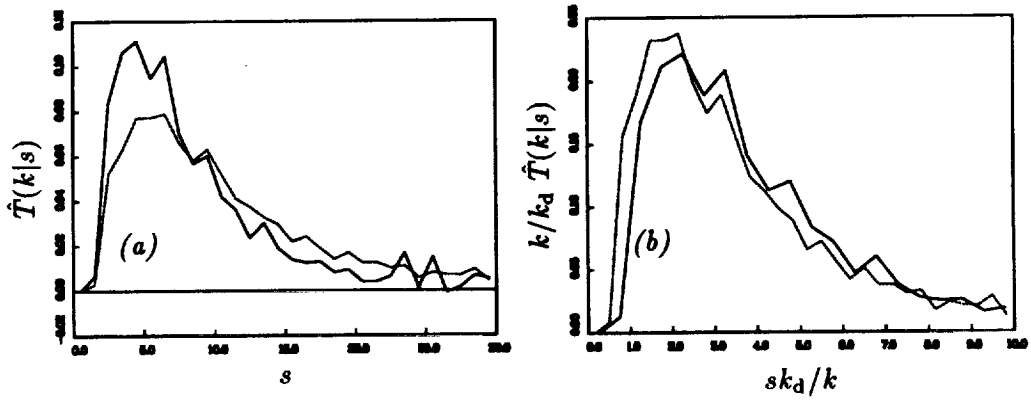

FIGURE 7. The scale disparity of energy transfer $\hat{T}(k|s)$: ——— , $k/k_d = 2$; ---- , $k/k_d = 3$. (a) local scaling: s, (b) non-local scaling sk_d/k.

energy spectrum function under the assumption that the fourth-order cumulants of the velocity are negligible:

$$T(k|p,q) = \theta_{kpq}\frac{Q^2}{16kpq}\Big((B_{kpq}+B_{kqp})\frac{E(p)E(q)}{p^2q^2} - B_{kpq}\frac{E(k)E(q)}{k^2q^2} - B_{kqp}\frac{E(k)E(p)}{k^2p^2}\Big), \tag{4.1}$$

where

$$B_{kpq} = (k^2-q^2)(p^2-q^2)+k^2p^2 \tag{4.2}$$

and

$$Q^2 = 2k^2p^2+2k^2q^2+2p^2q^2-k^4-p^4-q^4. \tag{4.3}$$

Here θ_{kpq}, the relaxation time of the triple moments of velocity, takes different forms in the various theories. In the far-dissipation range ($k,p,q \gg k_d$), however, it has the common expression

$$\theta_{kpq} = \frac{1}{\nu(k^2+p^2+q^2)}. \tag{4.4}$$

In the far-dissipation range of statistically stationary turbulence, the first two terms balance in (2.13),

$$T(k) = 2\nu k^2 E(k). \tag{4.5}$$

In this section, we omit the hat ($\hat{}$) because we are considering the continuous limit (infinite size of the periodic cube). The summation in (2.15) of the energy transfer function converts into the integral

$$T(k) = \int\int_{\Delta_k} T(k|p,q)\mathrm{d}p\mathrm{d}q, \tag{4.6}$$

where the integration is carried out under the condition that the three wavenumbers k, p, and q constitute a triangle.

C-2

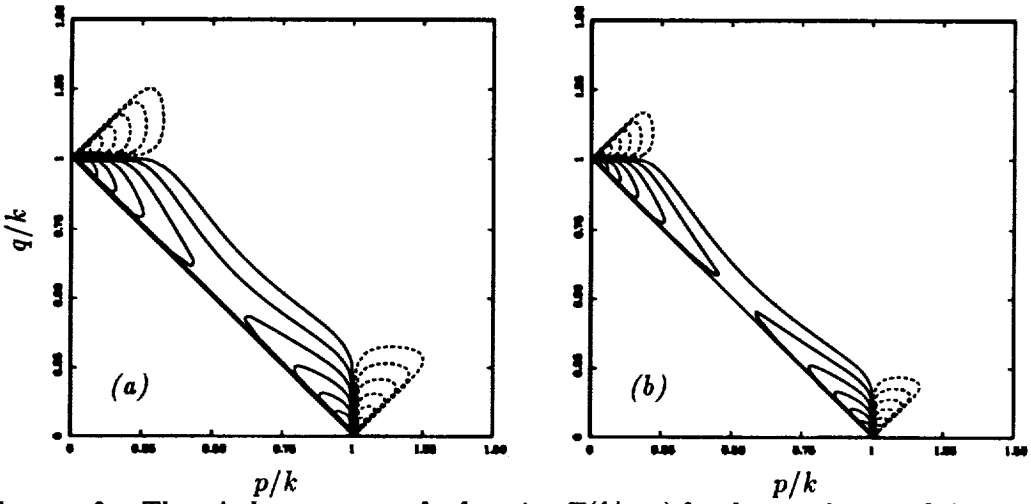

FIGURE 8. The triad energy transfer function $T(k|p,q)$ for the quasi-normal closure theory with $E(k) \propto (k/k_d)^{-1.6}\exp[-4.9k/k_d]$. (a) $k/k_d = 2$ and (b) $k/k_d = 3$. The solid and broken curves represent the positive and negative parts, respectively. The contour levels are logarithmic, rather than linear, and are separated by a factor of 4.

By substituting (4.6) with (4.1)-(4.4) and (3.3) into (4.5) and taking the leading terms in the limit of large wavenumber $k \gg k_d$, we obtain $\alpha = 3$ (Tatsumi 1980). This value of α is not consistent with the results of the numerical simulation as mentioned in section 3. The reason for this discrepancy is not known at present. As will be discussed in the next section, other values are consistent with the theory if the relaxation time θ_{kpq} is suitably modified (see (5.1)). We therefore proceed to examine the behavior of the triad energy transfer function expressed as (4.1) for the spectrum (3.3) with $\alpha = -1.6$.

In figure 8, we show the contours of $T(k|p,q)$ expressed by (4.1) with the spectrum (3.3) with $\alpha = -1.6$ and $\beta = 4.9$ for both $k/k_d = 2$ and $k/k_d = 3$. Contrary to the simulation data (figure 4), we can see contour lines at very low levels clearly. The same characteristics of $T(k|p,q)$ observed in figure 4 are also observed here. That is, (i) there are strong dipoles at the corners of the boundary of the triangle condition, (ii) $T(k|p,q)$ is positive where either p or q is less than k and negative otherwise, (iii) the magnitude of $T(k|p,q)$ decreases rapidly as point (p,q) moves away from the boundary $p+q=k$, and (iv) it decreases more rapidly as k/k_d increases. Moreover, the shape of the contours in figures 4 and 8 is very similar. The agreement is better for positive contours than for negative ones.

The difference in the shape of the contours can be seen more clearly in figure 9, which is an enlargement of figure 8 near $q \ll p \approx k$. As will be discussed in the next subsection, the slight difference in the shape of contours seems to be the main reason for the discrepancy in the behavior of $T(k|s)$ between the numerical simulation and the closure theory.

It should be mentioned here that the influence of the forcing term may not be

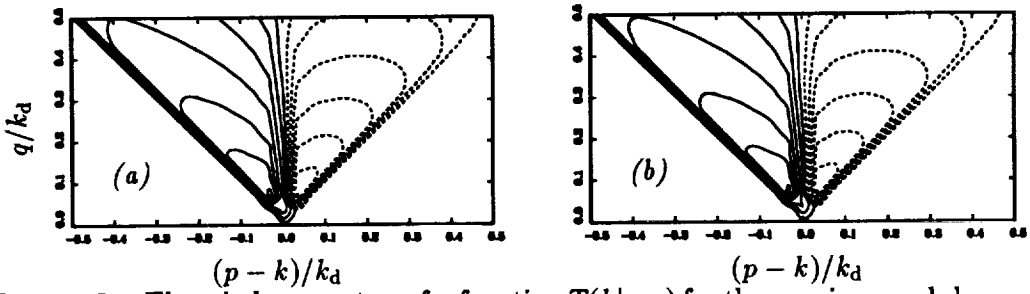

FIGURE 9. The triad energy transfer function $T(k|p,q)$ for the quasi-normal closure theory with $E(k) \propto (k/k_d)^{-1.6}\exp[-4.9k/k_d]$. (a) $k/k_d = 2$ and (b) $k/k_d = 3$. The solid and broken curves represent the positive and negative parts, respectively. The contour levels are logarithmic, rather than linear, and are separated by a factor of 4.

negligibly small. Since the fluid is forced at wavenumbers less than 3, the contours at $q/k_d < 0.1$ are directly affected by the forcing term.

So far, we have examined only the case of $\alpha = -1.6$. In order to see the dependence of $T(k|p,q)$ on the value of α, we plot in figure 10 the contours of $T(k|p,q)$ for various values of α ranging from 3 to -2. It is seen that the domains of the positive and negative parts are insensitive to the value of α, but the shape of the contours other than the zero level changes depending on the value of α. For a large value of α, the positive and negative peaks of $T(k|p,q)$ are far from the corners. They move toward the corner as α decreases. For $\alpha > 0$, the peaks are away from the corner, but for $\alpha < 0$, a positive and a negative peak merge into a dipole at the corner (see (4.12)). As will be shown in the next subsection, the dominant interactions in the energy transfer are local for $\alpha > 1$ and nonlocal for $\alpha < 1$.

4.1 Scale Disparity of Energy Transfer

Let $T(k|s)\mathrm{d}s$ be the contribution to the energy transfer to Fourier modes at wavenumber k due to triad interactions for which the scale disparity parameter lies between s and $s + \mathrm{d}s$. The contribution from all the triad interactions of scale disparity less than s is then written as

$$\int_1^s T(k|s')\mathrm{d}s' = \int \int_{\substack{\Delta_k \\ \frac{\max(k,p,q)}{\min(k,p,q)} \le s}} T(k|p,q)\mathrm{d}p\mathrm{d}q. \tag{4.7}$$

The derivative of (4.7) gives the scale disparity of energy transfer

$$T(k|s) = \frac{\mathrm{d}}{\mathrm{d}s} \int \int_{\substack{\Delta_k \\ \frac{\max(k,p,q)}{\min(k,p,q)} \le s}} T(k|p,q)\mathrm{d}p\mathrm{d}q. \tag{4.8}$$

The integration of $T(k|s)$ over all s gives the energy transfer $T(k)$, i.e.

$$T(k) = \int_1^\infty T(k|s)\mathrm{d}s. \tag{4.9}$$

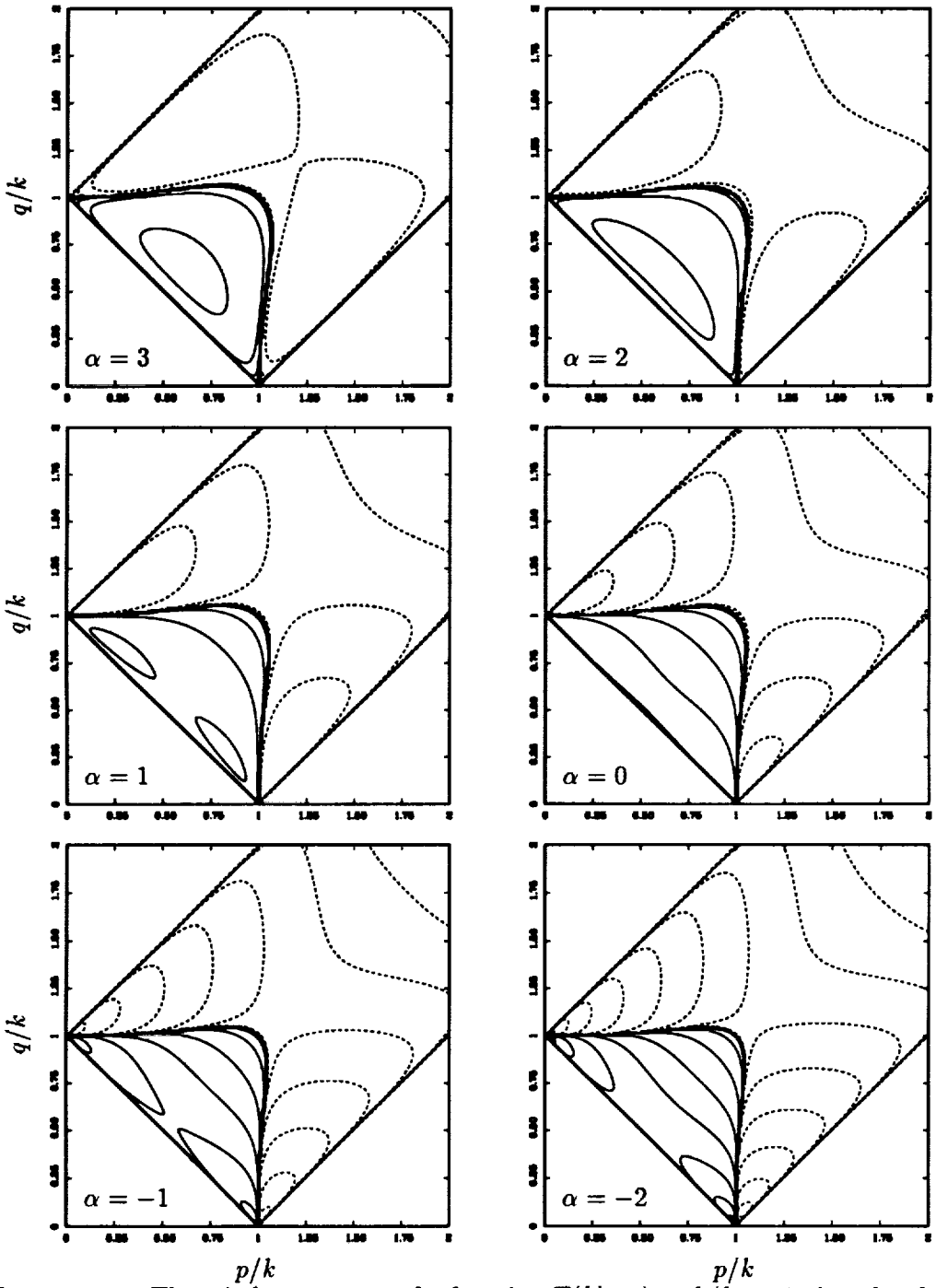

FIGURE 10. The triad energy transfer function $T(k|p,q)$ at $k/k_{\rm d} = 1$ given by the quasi-normal closure theory for $E(k) \propto (k/k_{\rm d})^{\alpha}\exp[-4.9k/k_{\rm d}]$, $-2 \leq \alpha \leq 3$

The integral (4.7) is written explicitly for $s \leq 2$ as (see figure 6)

$$\int_1^s T(k|s')\mathrm{d}s' = 2\left\{\int_{k/s}^{k}\mathrm{d}p\int_{k/s}^{p}\mathrm{d}q + \int_{k}^{sk}\mathrm{d}p\int_{p/s}^{p}\mathrm{d}q\right\}T(k|p,q) \qquad (4.10a)$$

and for $s \geq 2$ as

$$\int_1^s T(k|s')\mathrm{d}s' = 2\left\{\int_{k/2}^{(s-1)k/s}\mathrm{d}p\int_{k-p}^{p}\mathrm{d}q + \int_{(s-1)k/s}^{k}\mathrm{d}p\int_{k/s}^{p}\mathrm{d}q + \int_{k}^{sk/(s-1)}\mathrm{d}p\int_{p/s}^{p}\mathrm{d}q + \int_{sk/(s-1)}^{sk}\mathrm{d}p\int_{p-k}^{p}\mathrm{d}q\right\}T(k|p,q) \qquad (4.10b)$$

Differentiating (4.10a) and (4.10b) with respect to s we obtain

$$T(k|s) = 2\left\{\frac{k}{s^2}\int_{k/s}^{k}T(k|p,k/s)\mathrm{d}p + k\int_{k}^{sk}T(k|sk,q)\mathrm{d}q + \frac{1}{s^2}\int_{k}^{sk}pT(k|p,p/s)\mathrm{d}p\right\} \qquad (s \leq 2) \qquad (4.11a)$$

$$= 2\left\{\frac{k}{s^2}\int_{(s-1)k/s}^{k}T(k|p,k/s)\mathrm{d}p + k\int_{(s-1)k}^{sk}T(k|sk,q)\mathrm{d}q + \frac{1}{s^2}\int_{k}^{sk/(s-1)}pT(k|p,p/s)\mathrm{d}p\right\} \qquad (s \geq 2) \qquad (4.11b)$$

By substituting the expression (4.1) for $T(k|p,q)$ from the quasi-normal closure theory with the energy spectrum (3.3) into (4.11a) and (4.11b), we can calculate $T(k|s)$ explicitly. The scale disparity transfer function behaves differently depending on the values of α and k/k_d. In figure 11(a), we plot $T(k|s)$ for $k/k_\mathrm{d} = 1$, 2, and 3 with $\alpha = 3$. The interaction is localized around $s = 2$. The peak of the scale disparity parameter moves little as k/k_d increases. In figure 11(b), we plot $T(k|s)$ for $k/k_\mathrm{d} = 1$, 2, and 3 with $\alpha = -1.5$. The interaction becomes more nonlocal as k/k_d increases, and the peak of the scale disparity parameter moves linearly with k/k_d for large k/k_d.

In order to examine the wavenumber dependence of the transfer function, we replot it in figure 11(c) against sk_d/k for $k/k_\mathrm{d} = 2$, 3, and ∞ (see below for $k/k_\mathrm{d} = \infty$). The scale disparity of the energy transfer seems to approach a universal form for large values of k/k_d. The approach is faster for large values of s.

As demonstrated in figure 10, the triad energy transfer function $T(k|p,q)$ for small α (see below (4.12) for the critical value) has a double peak at the corners $q \ll p \approx k$ and $p \ll q \approx k$. This peak becomes steeper for larger values of k/k_d because of the exponential decay of the energy spectrum. This enables us to make

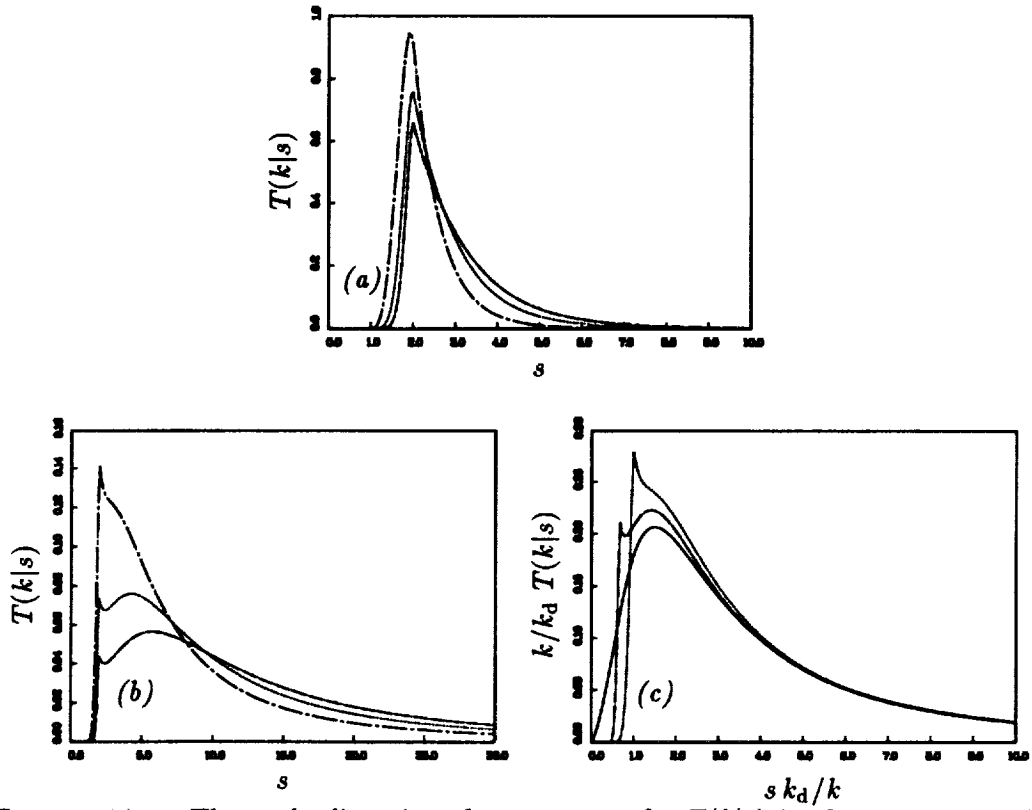

FIGURE 11. The scale disparity of energy transfer $T(k|s)$ in the quasi-normal closure theory with $E(k) \propto (k/k_\mathrm{d})^\alpha \exp[-4.9k/k_\mathrm{d}]$. (a) $\alpha = 3$, (b,c) $\alpha = -1.5$. ——— , $k/k_\mathrm{d} = 1$; - - - - , $k/k_\mathrm{d} = 2$; —·— , $k/k_\mathrm{d} = 3$; ——— , $k/k_\mathrm{d} = \infty$.

a local analysis around the corner to estimate the asymptotic behavior of $T(k|s)$ for large values of k/k_d. The triad energy transfer function (4.1) with the energy spectrum (3.3) behaves around $q \ll p \approx k$ as

$$T(k|p,q) = \frac{A^2}{4\nu}\left(\frac{k}{k_\mathrm{d}}\right)^\alpha \mathrm{e}^{-\beta k/k_\mathrm{d}} \left(\frac{q}{k_\mathrm{d}}\right)^\alpha q^{-3}(q^2-(p-k)^2)\mathrm{e}^{-\beta q/k_\mathrm{d}}\left(\mathrm{e}^{\beta(k-p)/k_\mathrm{d}}-1\right). \tag{4.12}$$

The energy transfer function $T(k)$ is calculated by integrating $T(k|p,q)$ with respect to p and q over the whole range. When $\alpha < 1$, the integral is localized at the corners $q \ll p \approx k$ and $p \ll q \approx k$ so that the asymptotic expression (4.12) can be used. The result is

$$\begin{aligned} T(k) &= 2\int_0^\infty \int_{k-q}^{k+q} T(k|p,q)\mathrm{d}p \\ &= \frac{2A^2 k_\mathrm{d}}{\nu\beta^{\alpha+1}}\left(\frac{2^{-2}}{(\alpha-2)(\alpha-1)}-\frac{1}{3}\right)\Gamma(\alpha+1)\left(\frac{k}{k_\mathrm{d}}\right)^\alpha \mathrm{e}^{-\beta k/k_\mathrm{d}} \end{aligned} \tag{4.13}$$

for $-2 < \alpha < 1$,where Γ is the Gamma function. Note that the integral is localized at the corners and converges only when $-2 < \alpha < 1$.

Substituting (4.12) into (4.11b), we obtain

$$T(k|s) = \frac{A^2 k_\mathrm{d}}{2\nu\beta^{\alpha+2}} \left(\frac{k}{k_\mathrm{d}}\right)^{\alpha-1} \mathrm{e}^{-\beta k/k_\mathrm{d}} \times \sigma^{-(\alpha+2)} \left(2\sigma^2(1-\sigma) - \tfrac{4}{3}\mathrm{e}^{-1/\sigma} + 2\sigma^2(1+\sigma)\mathrm{e}^{2/\sigma}\right), \quad (4.14)$$

where

$$\sigma = \frac{k_\mathrm{d}}{\beta k} s. \quad (4.15)$$

Note that we consider here the case $k/k_\mathrm{d} \gg 1$ so that $s \gg 1$ for a finite value of σ. The asymptotic form (4.14) of $T(k|s)$ for large values of k/k_d is drawn for $\alpha = -1.5$ and $\beta = 4.9$ in figure 11(c).

5. Discussion

The triad interaction in the dissipation range has been investigated by analysis of numerical turbulence data and the quasi-normal closure theory of turbulence. The results of the numerical simulation suggest that the motion at the Kolmogorov dissipation scale couples directly with the smaller scales and that the triad interaction is nonlocal in scale, at least in the wavenumber range $0.1 < k/k_\mathrm{d} < 4$ investigated here. The closure theory, on the other hand, suggests that the locality of the triad interaction depends crucially on the power α of an algebraic prefactor of the exponential decay of the energy spectrum at large wavenumbers. It is local or nonlocal for $\alpha > 1$ or $\alpha < 1$, respectively.

In the EDQNM and related quasi-normal closure theories, the triad energy transfer function is expressed by (4.1). The form of the relaxation time θ_{kpq} differs from theory to theory but has the common asymptotic form (4.4) in the far-dissipation range where a balance between energy transfer and dissipation requires $\alpha = 3$ instead of the value $\alpha \approx -1.6$ found in the numerical simulation.

It is interesting, however, to note that if the relaxation time is assumed to be independent of the wavenumber in the far dissipation range, say equal to the Kolmogorov time scale

$$\theta_{kpq} \propto \sqrt{\nu/\epsilon} = \frac{1}{\nu k_\mathrm{d}^2}, \quad (5.1)$$

then any value of α (including $\alpha = -1.6$) is compatible with the energy balance equation (4.4). As shown below, however, this is not the case in the EDQNM theory.

In the EDQNM theory, the relaxation time takes the form

$$\theta_{kpq} = \frac{1}{\nu(k^2+p^2+q^2) + \mu(k) + \mu(p) + \mu(q)}, \quad (5.2)$$

where $\mu(k) = \lambda(\int_0^k r^2 E(r)\mathrm{d}r)^{1/2}$ is the eddy damping rate and λ is an adjustable constant which may be related to the Kolmogorov constant C_K as $\lambda = 0.154 C_\mathrm{K}^{3/2}$

(André & Lesieur 1977). Note that $\lambda = 0.37$ for $C_K = 1.8$. The first term in the denominator in (5.2) represents viscous damping and the second the relaxation by straining motions of comparable and larger scales. The relaxation time has the following asymptotic forms for small and large wavenumbers for $C_K = 1.8$:

$$\theta_{kpq} = \frac{2.3}{k^{2/3} + p^{2/3} + q^{2/3}} \qquad (k, p, q \ll k_d) \tag{5.3a}$$

$$= \frac{1}{\nu(k^2 + p^2 + q^2)} \qquad (k, p, q \gg k_d) \tag{5.3b}$$

The integrals in (5.2) tend to the energy dissipation for large wavenumber,

$$\epsilon/2\nu = \int_0^\infty r^2 E(r)\mathrm{d}r. \tag{5.4}$$

The peak of the integrand lies around $r = 0.15k_d$, and the majority of the integrand is covered in the wavenumber domain $r < 0.5k_d$ (see Kida & Murakami 1987). The two effects are comparable at wavenumber

$$k, p, q \approx \lambda^{1/2}/2^{1/4}k_d \approx 0.5k_d. \tag{5.5}$$

Around these wavenumbers the relaxation time is written as

$$\theta_{kpq} \approx \frac{1}{\nu(k^2 + p^2 + q^2) + 0.78(\epsilon/\nu)^{1/2}} = \frac{1}{\nu(k^2 + p^2 + q^2 + 0.78{k_d}^2)}. \tag{5.6}$$

We may conclude from (5.3) and (5.6) that there is no region of constant θ_{kpq} in the EDQNM theory.

It is possible that the value of $\alpha \approx -1.6$ observed in wavenumber range $0.1 < k/k_d < 4$ is simply a tangent and that it approaches 3 in the limit of large wavenumbers. If so, the transfer may be dominated there by local triad interactions.

REFERENCES

ANDRÉ, J. C. & LESIEUR, M. 1977 Influence of helicity on the evolution of isotropic turbulence at high Reynolds number. *J. Fluid Mech.* **81**, 187.

DOMARADZKI, J. A. 1988 Analysis of energy transfer in direct numerical simulations of isotropic turbulence. *Phys. Fluids.* **31**, 2747.

DOMARADZKI, J. A. & ROGALLO, R. S. 1990 Local energy transfer and nonlocal interactions in homogeneous isotropic turbulence. *Phys. Fluids A.* **2**, 413.

KERR, R. M. 1990 Velocity, scalar and transfer of spectra in numerical turbulence. *J. Fluid Mech.* **211**, 309.

KIDA, S. & MURAKAMI, Y. 1987 Kolmogorov similarity in freely decaying turbulence. *Phys. Fluids.* **30**, 2030.

KIDA, S., MURAKAMI, Y., OHKITANI, K. & YAMADA, M. 1990 Energy and flatness spectra in a forced turbulence. *J. Phys. Soc. Japan.* **59**, 4323.

KOLMOGOROV, A. N. 1941 The local structure of turbulence in incompressible viscous fluid for very large Reynolds numbers. *C. R. (Dokl.) Acad. Sci. USSR.* **30**, 301.

KRAICHNAN, R. H. 1959 The structure of isotropic turbulence at very high Reynolds numbers. *J. Fluid Mech.* **5**, 497.

KRAICHNAN, R. H. 1971 Inertial-range transfer in two- and three-dimensional turbulence. *J. Fluid Mech.* **47**, 525.

LESIEUR, M. 1987 *Turbulence in Fluids.* Martinus Nijhoff.

OHKITANI, K. & KIDA, S. 1992 Triad interaction in a forced turbulence. *Phys. Fluids A.* **4**, 794.

ROGALLO, R. S. 1981 Numerical experiments in homogeneous turbulence. *NASA TM-81315.*

SANADA, T. 1992 Comment on the dissipation-range spectrum in turbulent flows. *Phys. Fluids A.* **4**, 1086.

SREENIVASAN, K. R. 1985 On the fine-scale intermittency of turbulence. *J. Fluid Mech.* **151**, 81.

TATSUMI, T. 1980 Theory of homogeneous turbulence. *Adv. Appl. Mech.* **20**, 39.

WALEFFE, W. 1992 The nature of triad interactions in homogeneous turbulence. *Phys. Fluids A.* **4**, 350.

YEUNG, P. K. & BRASSEUR, J. G. 1991 The response of isotropic turbulence to isotropic and anisotropic forcings at large scales. *Phys. Fluids A.* **3**, 884.

ZHOU, Y. 1992 Interacting scales and energy transfer in isotropic turbulence. (Submitted for publication.)